

1
2
3
4
5
6
7
8
9
10
11
12
13
14
15
16
17
18
19
20
21
22

Murine polyomavirus microRNAs promote viuria during the acute phase of infection

James M. Burke¹, Clovis R. Bass¹, Emin T. Ulug¹, Christopher S. Sullivan^{1,*}

*Correspondence:

Chris_sullivan@austin.utexas.edu

¹The University of Texas at Austin, Center for Systems and Synthetic Biology, Center for Infectious Disease and Dept. Molecular Biosciences, 1 University Station A5000, Austin TX 78712-0162

Running title: Polyomavirus miRNAs promote acute viuria

Keywords: Polyomavirus, miRNA, viral shedding, viral persistence

Abstract word count: 183

Manuscript word count: 4,103

23 **Abstract**

24 **Polyomaviruses (PyVs) can cause serious disease in immunosuppressed hosts. Several**
25 **pathogenic PyVs encode microRNAs (miRNAs), small RNAs that regulate gene expression**
26 **via RNA silencing. Despite recent advances in understanding the activities of PyV miRNAs,**
27 **the biological functions of PyV miRNAs during *in vivo* infections are mostly unknown.**
28 **Studies presented here use murine polyomavirus (MuPyV) as a model to assess the roles of**
29 **the PyV miRNAs in a natural host. This analysis reveals that a MuPyV mutant that is unable**
30 **to express miRNAs has enhanced viral DNA loads in select tissues at late times after**
31 **infection, indicating that during infection of a natural host, PyV miRNAs function to reduce**
32 **viral replication during the persistent phase of infection. Additionally, MuPyV miRNAs**
33 **promote viuria during the acute phase of infection as evidenced by a defect in shedding**
34 **during infection with the miRNA mutant virus. The viuria defect of the miRNA mutant virus**
35 **could be rescued by infecting Rag2^{-/-} mice. These findings implicate miRNA activity in both**
36 **the persistent and acute phases of infection and suggest a role for MuPyV miRNA in evading**
37 **the adaptive immune response.**

38

39 **Importance**

40 **MicroRNAs are expressed by diverse viruses, but for only a few is there any understanding**
41 **of their *in vivo* function. PyVs can cause serious disease in immunocompromised hosts.**
42 **Therefore, increased knowledge of how these viruses interact with the immune response is**
43 **of possible clinical relevance. Here we show a novel activity for a viral miRNA in promoting**
44 **virus shedding. This work indicates that in addition to any role for the PyV miRNA in long-**
45 **term persistence, that it also has biological activity during the acute phase. As this mutant**
46 **phenotype is alleviated by infection of mice lacking an effective adaptive immune response,**
47 **our work also connects the *in vivo* activity of a PyV miRNA to the immune response. Given**
48 **that PyV-associated disease is associated with alterations in the immune response, our**
49 **findings may help to better understand how the balance between PyV and the immune**
50 **response becomes altered in pathogenic states.**

51

52 **Introduction**

53

54 The polyomavirus (PyV) family is comprised of a large number of viruses that predominantly
55 infect vertebrates (1). The founding member of the PyVs, murine polyomavirus (MuPyV), has
56 been the most tractable *in vivo* model for studying the PyV life cycle and has played an important
57 role in understanding PyV-mediated transformation and the antiviral response (2, 3, 4). MuPyV is
58 thought to be transmitted to newborn mice via a respiratory route (5, 6, 7). Primary replication,
59 which occurs 1-6 days post-infection in nonciliated epithelial clara cells of the lungs (7), is
60 followed by dissemination and replication in secondary tissues 7-12 days post infection (6, 8).
61 Viral replication has been observed in various secondary organs, including kidneys, salivary
62 glands, spleen, lymph nodes, heart, liver, skin, lungs, and mammary glands (8, 9, 10). Virus
63 replication peaks around 12 days after infection, concurrent with a rise in viral shedding in the
64 urine and saliva (6). A rise in anti-MuPyV antibody titers occurs 7-15 days p.i. and precedes
65 clearance of detectable virus in most organs by 22-30 days (8).

66

67 A reduction in viral loads marks the transition from the acute phase to the persistent phase, which
68 is generally defined by the continued presence of viral DNA in tissues (3). Viral DNA is
69 maintained in select tissues, such as bone marrow, spleen, kidney, salivary glands, and mammary
70 glands (8, 9). The viral DNA in these tissues is thought to represent a persistent reservoir of
71 ‘smoldering’ viral replication in semi-permissive cells (4), although a latent state has yet to be
72 ruled out. A change in the microenvironment (e.g. tissue damage), immune status (e.g. pregnancy
73 or immunosuppression), or hormone levels (e.g. pregnancy, stress), can ‘reactivate’ or increase
74 replication of MuPyV from persistent reservoirs (11, 12). This results in episodic shedding of

75 MuPyV in urine and saliva, which contaminates the surrounding environment with infectious virus
76 (6). Similar observations have been made for human PyVs, whereby increased viuria during
77 pregnancy coincides with a rise in anti-PyV neutralizing antibodies (13, 14, 15).

78
79 Many polyomaviruses – including MuPyV, RacPyV, SV40, JCPyV, MCPyV, and BKPyV –
80 encode microRNAs (miRNAs) (16, 17, 18, 19, 20), small regulatory RNAs (~22 nt) that repress
81 gene expression via RNA silencing (21). The PyV miRNAs are encoded in the late orientation,
82 opposite to the T antigen mRNAs. Consequently, miRNAs are perfectly complementary to the T
83 antigen transcripts, permitting Argonaute 2 (Ago2)-mediated cleavage of these mRNAs. This
84 results in a reduction in T antigen protein levels late in infection, a conserved function of PyV
85 miRNAs (16, 17, 18, 19, 20, 22). Despite established roles of T antigen in promoting viral
86 replication, miRNA-null laboratory strains of SV40 and MuPyV replicate at rates similar to their
87 wild type counterparts under standard cell culture conditions (16, 17). However, miRNAs
88 expressed by non-rearranged BKPyV strains, which more closely resemble circulating BKPyV in
89 humans and express lower levels of the early transcripts, are able to downregulate T antigen levels
90 to sufficiently reduce viral replication in primary renal proximal tubule epithelial cells (23).
91 Consistent with these results, MCPyV miRNA promotes long-term persistence by inhibiting DNA
92 replication in a cell culture model (24), and the SV40 miRNAs reduce persistent SV40 DNA loads
93 in Syrian Golden hamster tissues (25). These studies suggest that the PyV miRNAs reduce virus
94 replication by down-regulating T antigen expression. However, the effects of miRNA expression
95 on virus replication in a natural host have yet to be established.

96

97 In addition to regulating viral replication, independent studies implicate a role for the PyV
98 miRNAs in inhibiting the host immune response. Downregulation of T-antigen by the SV40
99 miRNAs decreases CD8 T-cell-mediated lysis in cell culture (16). miRNA-mediated
100 downregulation of the host ULBP3 stress-induced ligand has been suggested to reduce killing of
101 BKV- and JCV-infected cells by natural killer cells (26). MuPyV miRNAs reduce Smad2-
102 mediated apoptosis during infection (27). These studies support a model whereby the PyV
103 miRNAs modulate viral and host transcripts in order to extend the life of infected cells by reducing
104 innate and adaptive immune responses.

105

106 Despite advances in understanding the expression and activities of PyV miRNAs, their functions
107 during the viral lifecycle in a natural host are poorly understood. In this study, we use MuPyV as
108 a model to investigate the role of PyV miRNAs on viral dissemination, replication, and shedding
109 during the acute and persistent phases of infection in mice. This work reveals activities of the
110 MuPyV miRNA in both the persistent and acute phases of infection and suggests a link between
111 miRNA function and the adaptive immune response.

112

113 **Results**

114

115 **Sequencing of the MuPyV miRNAs**

116 MuPyV miRNAs were initially identified via secondary structure predictions and confirmed
117 indirectly (17). This approach could only estimate the 5' and 3' termini of the derivative miRNAs.
118 It also did not resolve whether MuPyV contains additional miRNA loci. To better characterize the
119 MuPyV miRNAs, we conducted high throughput sequencing of small RNA from NIH3T3 cells
120 infected with the MuPyV PTA strain (Figure 1). These results map with precision the termini of
121 the MuPyV miRNAs and confirm that only the single, previously identified pre-miRNA locus,
122 gives rise to MuPyV-encoded miRNA derivatives.

123

124 **MuPyV miRNAs correlate with reduced viral DNA loads during the persistent phase of**
125 **infection.**

126 PTA-dll013 is a deletion mutant of the MuPyV-PTA strain that does not express miRNAs (17).
127 Previous studies reported that adult C57BL/6 mice infected with PTA-dll013 maintained
128 comparable or slightly higher (up to 5-fold) vDNA loads as compared to PTA in spleen and kidney
129 during the acute phase of infection (up to 34 days p.i.) (17). To confirm these results and determine
130 whether the miRNA function at later times post-infection, we examined MuPyV DNA loads by
131 qPCR in spleens, kidneys, and livers of adult C57BL/6 mice infected with 10^5 IU of PTA or PTA-
132 dl1013 via IP injection during the acute (1 and 4 weeks p.i.) and persistent (10, 16, and 28 weeks
133 p.i.) phases of infection (Figure 2).

134

135 High virus yields (2×10^5 - 5×10^6 genome equivalents/ug DNA) were observed in spleen and
136 kidney after one and four weeks of infection with PTA, consistent with robust virus replication
137 during the acute phase of replication (Figure 2). Lower levels were observed in liver during these
138 times (Figure 2). Virus loads diminished to $\leq 10^3$ genome equivalents/ug DNA at later times after
139 infection (16 and 28 weeks p.i.), consistent with a low level of virus replication during the
140 persistent phase of replication. These levels were only slightly above the limit of detection of our
141 PCR assay, even when increased input DNA was assayed.

142

143 In comparison to PTA, PTA-dl1013 levels were 4.1-fold lower in spleen, but not kidney, at one
144 week p.i. (Figure 2, closed symbols). No significant differences in PTA and PTA-dl1013 DNA
145 levels were detected at 4 weeks or 10 weeks after infection. However, at 16 weeks, PTA-dl1013
146 genome levels were approximately 10-fold higher than PTA in spleen and kidney. By 28 weeks,
147 only low levels of both PTA and PTA-dl1013 genome levels were detected and no significant
148 differences were observed. These results confirm that the miRNAs are not required for infection
149 and replication in tissues during the acute phase of infection, and indicate that miRNA expression
150 correlates with reduced genomic DNA in certain tissues during the persistent phase of infection.

151

152 The results summarized in Figure 2 reveal a substantial variation in viral copies between different
153 mice. To minimize variations due to inter-host differences, we compared levels of PTA and PTA-
154 dl1013 in individual animals. C57BL/6 mice were co-infected with equivalent amounts of PTA
155 and PTA-dl1013 by IP injection. Tissues were then harvested during the acute (2 and 4 weeks) and
156 persistent (10 and 16 weeks) phases of infection, and genome levels were determined by strain-
157 specific qPCR (Supplemental Figure 1A-C). Similar to individually infected mice, we observed

158 high levels of both PTA and PTA-dl1013 in tissues during the acute phase of infection, with
159 MuPyV levels decreasing during the persistent phase of infection (Figure 3). We note that PTA
160 was not detected in the spleen or kidney by 16 weeks p.i., while PTA-dl1013 was present at 10^3 -
161 10^4 copies/ug DNA (Figure 3). To compensate for variation in different animals, we calculated the
162 ratio of PTA to PTA-dl1013 genomes in individual mice. This analysis reveals that during the
163 acute phase of infection (2 and 4 weeks p.i.), the levels of PTA and PTA-dl1013 were comparable
164 in spleen and kidney (Figure 4). At later times, PTA-dl1013 copy numbers were 10-fold higher
165 than PTA in the spleen and kidney at weeks 10 and 16 and 100-fold higher in the kidney at week
166 16 (Figure 4). We did not observe substantial differences in the liver, but did observe 7-fold higher
167 PTA-dl1013 in the bladder at week 4 (Figure 4). These results are consistent with the elevated
168 levels of PTA-dl1013 detected in the spleen and kidney at 16 weeks following infections with the
169 individual virus strains (Figure 2) and suggest that MuPyV miRNA expression correlates with
170 reduced viral loads in select tissues during the persistent phase of infection.

171

172 **MuPyV miRNAs promote viuria during the acute phase of infection.**

173 Early epidemiological studies of MuPyV revealed that high titers of infectious virus are excreted
174 in the urine of mice during the acute phase of infection and then episodically shed during the
175 persistent phase of infection (6). The periodic shedding of MuPyV and many other PyVs in the
176 urine is considered a primary route of transmission (6,28). Therefore, we investigated whether the
177 MuPyV miRNAs affects the magnitude and/or frequency of MuPyV shedding in the urine during
178 the acute and persistent phases of infection. To test this, we collected urine specimens periodically
179 post-infection and quantitated viral genomes. To assess whether PTA-dl1013 could maintain long-

180 term persistence, we treated mice with cyclosporine at day 474 post-infection in order to
181 immunosuppress the mice, which is correlated with increased PyV replication (4).

182

183 In the majority of mice individually infected with PTA or PTA-dl1013, we observed vDNA
184 shedding of both strains during the acute phase of infection (13-34 days p.i.) (Supplemental Figure
185 2), indicating that the MuPyV miRNAs are not required for establishing viuria. Both strains were
186 episodically shed throughout the persistent phase (34-87 day p.i.), which demonstrates that the
187 MuPyV miRNAs are not required for persistent viuria (Supplemental Figure 2). The magnitude
188 and timing of virus shedding by individual mice infected varied substantially (Supplemental Figure
189 2), and thus no statistical differences between PTA and PTA-dl1013 levels could be determined.

190

191 To circumvent the differences in shedding due to variations between individual mice, we tested
192 whether expression of miRNA could correlate with viral shedding in mice co-infected with both
193 PTA and PTA-dl1013. Adult C57BL/6 female mice were co-infected with equal amounts of the
194 PTA and PTA-dl1013, and PTA and PTA-dl1013 DNA was quantitated during the acute and
195 persistent phases of infection (Figure 5A). We did not detect substantial quantities of either PTA
196 or PTA-dl1013 genomes in the urine of ~40% of the mice at any time point during the acute phase
197 of infection (Supplemental file). The remaining “high-shedder” mice expressed readily detectable
198 MuPyV DNA in the urine. MuPyV in these samples was detected at high levels beginning by 10
199 days p.i. and peaked between 13-27 days, after which the number of shedding mice and the
200 magnitude of shedding began to decrease. Thereafter, we observed episodic shedding events
201 throughout the persistent phase of infection (34-87 days p.i.). These findings reveal that while

202 some mice rarely or never shed detectable virus under our assay conditions, ~60% that are
203 competent for acute and persistent viuria.

204

205 The median PTA levels were significantly higher (5- to 100- fold) than PTA-dl1013 during the
206 majority of the acute phase of infection (10, 13, 15, 17, 20 and 27 days p.i.) in co-infected mice
207 (Figure 5A). To minimize the variance in individual mice, we determined the ratio of PTA:PTA-
208 dl1013 DNA in each individual mouse. This data confirmed that PTA was shed at significantly
209 higher levels on average (~10-fold) than PTA-dl1013 during days 10-17 of the acute phase of
210 infection in individual mice co-infected mice (Figure 5B). We did not observe statistically
211 significant differences in the magnitude of viral shedding at the majority of times tested during the
212 persistent phase of infection (Figure 5A, 5B, Supplemental file). Although this may be due to high
213 variance in the timing and the magnitude of shedding, as well as the lower number of mice tested,
214 this suggests that the MuPyV miRNAs do not promote viuria during the persistent phase of
215 infection. In fact, we observed eighty-four PTA-dl1013 shedding events that were above the limit
216 of detection from days 34 through 87, compared to thirty-three for PTA (Figure 5A). This implies
217 that the MuPyV miRNAs may limit detectable shedding during persistent phase of infection,
218 consistent with the reduced PTA levels in tissues (Figures 2-4). At late times post-infection (467-
219 492), we observed PTA and PTA-dl1013 shedding events in a small number of mice. Thus, the
220 MuPyV miRNAs are not required to maintain long-term persistent infections. These data further
221 indicate that the MuPyV miRNAs promote viral shedding during the acute phase of infection, but
222 limit the number of MuPyV shedding event during the persistent phase of infection.

223

224

225 **The shedding defect of miRNA-null MuPyV is mitigated in Rag2^{-/-} mice.**

226 The host immune response plays an important role in controlling MuPyV infection (2-4), and two
227 lines of evidence suggest that PyV miRNAs may function to reduce the adaptive immune response.
228 First, miRNA-mediated down-regulation of T-antigens decreases susceptibility to cytotoxic T-
229 cell-mediated lysis to SV40-infected cultured cells (16). Second, miRNA-null strains of SV40 and
230 JCV have only been isolated from severely immunocompromised hosts, suggesting that an active
231 immune response provides selective pressure to maintain miRNA expression (29). Since the
232 absence of the MuPyV miRNA results in decreased virus shedding during the acute phase of
233 infection, we tested whether the defect in acute viral shedding of PTA-dl1013 is mitigated in
234 C57BL/6 Rag2^{-/-} mice, which lack mature T- and B- cells. C57BL/6 Rag2^{-/-} mice were co-
235 infected with PTA and PTA-dl1013, and the shedding of DNA in urine was monitored. Unlike
236 wild type mice, where ~40% of animals did not shed detectable vDNA during the acute phase of
237 infection, all infected C57BL/6 Rag2^{-/-} mice shed detectable levels of MuPyV by 10 days post-
238 infection (Figure 6 and Supplemental file). Levels of both PTA and PTA-dl1013 DNA in urine
239 were found to continually increase in the co-infected C57BL/6 Rag2^{-/-} mice up to 20 days p.i.,
240 whereas MuPyV levels leveled off and began to decrease by 20 days p.i. (Figure 6). These
241 observations are consistent with the host adaptive immune response being a major factor that
242 controls MuPyV shedding. Importantly, unlike in wild type C57BL/6 mice, C57BL/6 Rag2^{-/-} mice
243 shed PTA-dl1013 DNA at levels similar to PTA during the acute phase of infection (10-13 days
244 p.i.) (Figure 6). These data indicate that the MuPyV miRNAs promote viuria during the acute
245 phase of infection in a manner that is dependent on the host having an intact adaptive immune
246 response.

247

248 **Discussion**

249

250 The natural *in vivo* functions of PyV miRNAs are poorly understood. Results presented here reveal
251 that, consistent with previous studies in cell culture models and a non-natural host (23-25), the
252 PyV miRNAs function to reduce viral loads during the persistent infection of a natural host. In
253 addition, we uncover novel effects of the MuPyV miRNAs on viuria during the persistent and
254 acute phases of infection that provide new insights into PyV miRNA biology.

255

256 Similar to previous studies (17), we did not observe large differences in the gross levels of PTA
257 (wild type) and PTA-dl1013 (miRNA-null) strains of MuPyV in tissues during acute phase of
258 infection (weeks 1, 2 and 4 p.i.). This further confirms that the MuPyV miRNAs are not required
259 for acute viral infection and replication *in vivo* under laboratory conditions. However, at weeks 10
260 and 16 p.i., we observed higher levels of PTA-dl1013 DNA, relative to PTA, in kidney and spleen
261 of mice following single- or co-infection with PTA and PTA-dl1013 (Figures 2-4). Similar
262 findings were observed in tissues of Syrian golden hamsters infected with miRNA-null strains of
263 the simian virus SV40 (25). These results are consistent with the notion that miRNA-mediated
264 downregulation of T antigen reduces virus replication in specific tissues/cell-types at late times
265 after infection to promote viral persistence (23,24).

266

267 Our assessment of MuPyV viuria revealed that the MuPyV miRNAs are not required to establish
268 or maintain long-term viral persistence (Figure 5 and Supplemental Figure 2). However, we did
269 observe more PTA-dl1013 than PTA shedding events during the persistent phase of infection (34-
270 87 days p.i.). This is consistent with increased PTA-dl1013 levels in tissues and further indicates

271 that the MuPyV miRNAs may limit viral replication events during the persistent phase of infection.
272 Though the function of this activity remains unclear, it may be important to prevent priming of the
273 host immune response in order to transmit to naïve hosts more efficiently. Alternatively, this
274 activity could prevent viral-associated pathologies to the host, which would presumably decrease
275 viral fitness. Future experiments will address the relevant role of miRNA-mediated reduction of
276 viral loads in urine and tissues during the persistent phase of infection.

277

278 During the acute phase of infection (days 10-20) in wild type C57BL/6 mice, only ~60% of mice
279 shed substantial levels of MuPyV DNA (Figure 5 and Supplemental Figure 2). This is in contrast
280 to infections in immunodeficient C57BL/6 *Rag2*^{-/-} mice, in which 100% of mice shed substantial
281 levels of MuPyV DNA. This suggests that the adaptive immune response is a major factor
282 controlling viuria. Analysis of wild-type C57BL/6 mice co-infected with PTA and PTA-dl1013
283 revealed that PTA-dl1013 DNA was shed at significantly lower levels than PTA (Figure 5), which
284 indicates the MuPyV miRNAs promote viral shedding at early times post-infection. Importantly,
285 the defect in PTA-dl1013 was largely mitigated during infection of immunodeficient C57BL/6
286 *Rag2*^{-/-} mice (Figure 6), suggesting that the MuPyV miRNAs help evade a component of the host
287 adaptive immune response to promote viuria. We note that PTA-dl1013 shedding was not fully
288 rescued by infecting C57BL/6 *Rag2*^{-/-} mice, possibly indicating that the MuPyV miRNAs have
289 additional activities [for example, reduction of smad2-mediated apoptosis (27)] in promoting
290 viuria independent of the adaptive immune response. These combined data demonstrate that the
291 MuPyV miRNAs promote viral shedding by at least indirectly interacting with the adaptive
292 immune response. This activity could be important in the wild as a means to increase transmission
293 of the virus to susceptible hosts during the acute phase of infection.

294

295 The exact mechanism(s) by which MuPyV miRNA expression enhances virus shedding in
296 immunocompetent mice remains unclear. Because we observed miRNA-dependent promotion of
297 shedding in co-infected immunocompetent mice, this indicates that MuPyV miRNAs are likely
298 functioning via a cell autonomous mechanism to repress the effects of the adaptive immune
299 response. This is consistent with previous findings that the SV40 miRNAs can reduce CD8 T-cell-
300 mediated lysis. However, it is unclear why the miRNAs promote viuria only during a narrow
301 window of time post-infection. One possibility is that the MuPyV miRNAs increase dissemination
302 to the target cells required for subsequent viuria, possibly by reducing the CTL response to promote
303 infection/replication in lymphocytes early during the acute phase of infection. In support of this,
304 at one week p.i., but not at 2 and 4 weeks p.i., we observed ~4-fold higher PTA DNA levels
305 specifically in the spleen (Figures 2-4), indicating the MuPyV miRNAs may promote infection of
306 lymphocytes early during infection. Alternatively, the cell-mediated adaptive immune response to
307 MuPyV may change over time, making the miRNAs less effective at promoting viuria. While the
308 CD8⁺ T cell response to MuPyV is predominately to T-antigen, the CD8⁺ T cell response has also
309 been shown to be directed toward a VP2-derived nonamer peptide (30). Thus, as the infection
310 progresses, miRNA-mediated down-regulate of T-antigens may become less effective at muting
311 the CTL response as the host T-cell response develops more so against the late VP proteins. Future
312 studies are required to more precisely define the relevant components of the immune response
313 important for hindering the miRNA mutant virus.

314

315 In summary, this study demonstrates functionality of MuPyV miRNAs during both the persistent
316 and acute phases of infection and at least indirectly implicates their function in altering some

317 component of the adaptive immune response. Given the clinical relevance of understanding the
318 interplay between polyomaviruses and the immune response, this work provides a useful,
319 quantitative, and non-invasive system for future efforts at understanding PyV miRNA effects on
320 adaptive immunity.

321

322 **Materials and Methods**

323

324 **Cell cultures and virus strains**

325 Primary baby mouse kidney (BMK) cell cultures were prepared from 2-4 week old female
326 C57BL/6 mice (Jackson Laboratories). Kidneys were excised, washed in PBS, and incubated in
327 DMEM containing 0.25% trypsin overnight at 4°C. Kidneys were homogenized, incubated in
328 trypsin at 37°C with agitation, and suspended in DMEM+10% FBS (Cellgro). Cells were washed
329 by centrifugation and plated at a density of 10^7 cells per 100 mm dish. NIH3T3 cells were
330 maintained in DMEM+10% FBS.

331

332 The PTA and PTA-dl1013 virus strains have been described previously (17). Virus was propagated
333 by infecting primary BMK cells (80% confluent) with PTA or PTA-dl1013 at an MOI of 0.05.
334 Virus stocks were prepared after 10 days by scraping the cells into a portion of the culture medium.
335 The cell extracts were then subjected to three freeze/thaw cycles, clarified by centrifugation, and
336 stored at -80°C.

337

338 Virus titers were determined by immunofluorescence. 80-90% confluent NIH3T3 cells in 12- or
339 24-well plates were infected with dilutions of the PTA and PTA-dl1013 virus stocks for one hour.
340 Infected cells were maintained in DMEM+2% FBS for 40 hours and then fixed and permeabilized
341 with 4% paraformaldehyde and 1% NP-40. After blocking with 10% goat serum overnight, cells
342 were incubated with rabbit-anti-PyV antibody (a gift from Dr. Richard Consigi) for 30 min. After
343 three PBS washes, cells were stained with Cy3-goat-anti-rabbit IgG (Abcam) for 10 min. and

344 washed. The numbers of total and stained cells per field were quantified by using an inverted
345 fluorescent microscope (Leica), and infectious titers (IU/ml) were determined.

346

347 **Animal infections and tissue analysis**

348 Female C57BL/6 (Jackson Laboratories) and C57BL/6 *Rag2*^{-/-} mice were inoculated with 1×10^5
349 IU of either PTA or PTA-dl1013 via intraperitoneal (IP) injection between 4 and 5 weeks of age.
350 For co-infections, mice were inoculated (IP) with 5×10^4 IU of PTA and 5×10^4 IU of PTA-
351 dl1013. Cyclospoin was administered as described in (31). Tissues were harvested at the indicated
352 times and flash frozen in liquid nitrogen. Homogenates were prepared by grinding with a mortar
353 and pestle chilled with liquid nitrogen. DNA was extracted from 25 mg of tissue by using the
354 DNeasy Blood and Tissue kit (Qiagen). Recovered DNA was quantitated by the Nanodrop
355 procedure and diluted to 100 ng/ul or 10 ng/ul for qPCR analysis.

356

357 **Urine analysis**

358 To collect urine, mice were placed on wire-bottomed cages for 2-4 hours. Urine was collected on
359 Parafilm, and 50 ul aliquots (or the total if less than 50 ul) were used for DNA extraction with the
360 QIAamp viral RNA mini kit (Qiagen) following the manufacturer's protocol to remove PCR
361 inhibitors. DNA was eluted in 60 ul of TE buffer. MuPyV copy numbers were normalized to that
362 in 2 ul of urine.

363

364 **Quantitative PCR**

365 Concentrated pBluescript-sk+PTA and pBluescript-sk+PTA-dl1013 vectors were obtained via
366 Maxi Prep (Invitrogen). Plasmids were prepared at 85.5 ng/ul (10^{10} copies of PTA or PTA-dl1013

367 per ul) and then serial diluted. For tissue analysis from individually infected mice, 20 ng of DNA
368 (for samples taken 1, 4, 10 weeks p.i.) or 200 ng of DNA (10 and 28 weeks p.i.) in 2 ul of TE
369 buffer was added to an 8 ul reaction mixture containing 5 ul of 2X gene expression master mix
370 (Applied Biosystems), 0.75 uM of MuPyV sense primer (CGCACATACTGCTGGAAGAAGA),
371 1.0 uM MuPyV antisense primer (TCTTGGTCGCTTTCTGGATACAG), and 100 nM of MuPyV
372 TaqMan MGB (Applied Biosystems) probe (FAM-ATCCTTGTGTTGCTGAGCCCGATGA-
373 NFQ) as described (32). For specific detection of PTA and PTA-dl1013 in urine, 2 ul of DNA (of
374 the 60 ul extracted unless otherwise indicated in Supplemental file) was added to an 8 ul reaction
375 mixture containing 5 ul 2X gene expression master mix (Applied Biosystems), 0.75 uM of
376 PTA/PTA-dl1013 sense primer (GATGAGCTGGGGTACTTGT), 0.75 uM of PTA/PTA-dl1013
377 antisense primer (TGTATCCAGAAAGCGACCAAG), and 100 nM of either the PTA-specific
378 TaqMan MGB (Applied Biosystems) probe (FAM-TAGGATGTCCAAATACAGATCCTC-
379 NFQ) or PTA-dl1013-specific TaqMan MGB (Applied Biosystems) probe (FAM-
380 CTCCGGTTCCATTGGCATGT-NFQ). The PTA and PTA-dl1013 standards (10^7 /ul - 10^1 /ul) were
381 confirmed by using the universal MuPyV primers/probe, which detects both PTA and PTA-
382 dl1013, to ensure that the copy number of each standard was equal. Assays were performed using
383 384-well format plates in a ViiA™ 7 Real-Time PCR System (Applied Biosystems). The limit of
384 detection was 10 copies.

385

386 **Statistical analyses**

387 One sample T-test (two-tailed) and Mann-Whitney U-test (two-tailed) were performed using real
388 statistics resource package for excel (<http://www.real-statistics.com/>).

389 **References**

- 390 1. Johne R, Buck CB, Allander T, Atwood WJ, Garcea RL, Imperiale MJ, Major EO, Ramqvist
391 T, Norkin LC. 2011. Taxonomical developments in the family Polyomaviridae. Arch Virol
392 156: 1627–1634.
- 393 2. Benjamin TL. 2001. Polyoma virus: old findings and new challenges. Virology 289: 167-173.
- 394 3. Ramqvist T, Dalianis T. 2009. Murine polyomavirus tumour specific transplantation antigens
395 and viral persistence in relation to the immune response, and tumour development. Semin
396 Cancer Biol 19: 236–243.
- 397 4. Swanson PA, Lukacher AE, Szomolanyi-Tsuda E. 2009. Immunity to polyomavirus infection:
398 The polyomavirus–mouse model. Semin Cancer Biol 19: 244-251.
- 399 5. Rowe WP, Hartley JW, Brodsky I, Huebner RJ, Law LW. 1958. Observations on the spread
400 of mouse polyoma virus infection. Nature 182:1617-16179.
- 401 6. Rowe W P. 1961. The epidemiology of mouse polyoma virus infection. Bacteriol Rev 25:18-
402 31.
- 403 7. Gottlieb K, Villarreal LP. 2000. The Distribution and Kinetics of Polyomavirus in Lungs of
404 Intranasally Infected Newborn Mice. Virology 266: 52-65.
- 405 8. Dubensky TW, Villarreal LP. 1984. The primary site of replication alters the eventual site of
406 persistent infection by polyomavirus in mice. J Virol 50: 541-546.
- 407 9. Wirth JJ, Amalfitano A, Gross R, Oldstone MB, Fluck MM. 1992. Organ- and age-specific
408 replication of polyomavirus in mice. J Virol 66:3278-86.

- 409 10. Berke Z, Dalianis T. 1993. Persistence of polyomavirus in mice infected as adults differs from
410 that observed in mice infected as newborns. *J Virol* 67: 4369-4371.
- 411 11. Atencio IA, Shadan FF, Zhou XJ, Vaziri ND, Villarreal LP. 1993. Adult mouse kidneys
412 become permissive to acute polyomavirus infection and reactivate persistent infections in
413 response to cellular damage and regeneration. *J Virol* 67: 1424–1432.
- 414 12. McCance DJ, Mims CA. 1979. Reactivation of polyoma virus in kidneys of persistently
415 infected mice during pregnancy. *Infect Immun* 25: 998–1002.
- 416 13. Coleman DV, Gardner SD, Mulholland C, Fridiksdottir V, Porter AA, Lilford R, Valdimarsson
417 H. 1983. Human polyomavirus in pregnancy. A model for the study of defense mechanisms to
418 virus reactivation. *Clin Exp Immunol* 53: 289-296.
- 419 14. Eash S, Manley K, Gasparovic M, Querbes W, Atwood WJ. 2006. The human polyomaviruses.
420 *Cell Mol Life Sci* 63:865-876.
- 421 15. Gibson PE, Field AM, Gardner SD, Coleman DV. 1981. Occurrence of IgM antibodies against
422 BK and JC polyomaviruses during pregnancy. *J Clin Pathol* 34: 674-679.
- 423 16. Sullivan CS, Grundhoff AT, Tevethia S, Pipas JM, Ganem D. 2005. SV40-encoded
424 microRNAs regulate viral gene expression and reduce susceptibility to cytotoxic T cells.
425 *Nature* 435: 682-686.
- 426 17. Sullivan CS, Sung CK, Pack CD, Grundhoff AT, Lukacher AE, Benjamin T, Ganem D. 2009.
427 Murine polyomavirus encodes a microRNA that cleaves early RNA transcripts but is not
428 essential for experimental infection. *Virology* 387: 157-167.
- 429 18. Seo GJ, Chen CJ, Sullivan CS. 2009. Merkel cell polyomavirus encodes a microRNA with the
430 ability to autoregulate viral gene expression. *Virology* 383: 183-187.

- 431 19. Seo GJ, Fink LH, O'Hara B, Atwood WJ, Sullivan CS. 2008. Evolutionarily conserved
432 function of a viral microRNA. *J Virol* 82: 9823-9828.
- 433 20. Chen CJ, Cox JE, Azarm K, Wylie KN, Woolard KD, Pesavento PA, Sullivan CS. 2015.
434 Identification of a Polyomavirus microRNA Highly Expressed in Tumors. *Virology* 476: 43–
435 53.
- 436 21. Bartel DP. 2004. MicroRNAs: genomics, biogenesis, mechanism, and function. *Cell* 116: 281-
437 297.
- 438 22. Chen CJ, Cox JE, Kincaid RP, Martinez A, Sullivan CS. 2013. Divergent MicroRNA
439 Targetomes of Closely Related Circulating Strains of a Polyomavirus. *J Virol* 87:11135-11147.
- 440 23. Broekema NM, Imperiale MJ. 2013. miRNA regulation of BK polyomavirus replication during
441 early infection. *Proc Natl Acad Sci U S A* 110: 8200-8205.
- 442 24. Theiss JM, Günther T, Alawi M, Neumann F, Tessmer U, Fischer N, Grundhoff A. 2015. A
443 Comprehensive Analysis of Replicating Merkel Cell Polyomavirus Genomes Delineates the
444 Viral Transcription Program and Suggests a Role for mcv-miR-M1 in Episomal Persistence.
445 *PLoS Pathog* 11:e1004974.
- 446 25. Zhang S, Sroller V, Zanwar P, Chen CJ, Halvorson SJ, Ajami NJ, Hecksel CW, Swain JL,
447 Wong C, Sullivan CS, Butel JS. 2014. Viral MicroRNA Effects on Pathogenesis of
448 Polyomavirus SV40 Infections in Syrian Golden Hamsters. *PLoS Pathog* 10: e1003912.
- 449 26. Bauman Y, Nachmani D, Vitenshtein A, Tsukerman P, Drayman N, Stern-Ginossar N, Lankry
450 D, Gruda R, Mandelboim O. 2011. An identical miRNA of the human JC and BK polyoma
451 viruses targets the stress-induced ligand ULBP3 to escape immune elimination. *Cell Host*
452 *Microbe* 9:93-102.

- 453 27. Sung SK, Yim H, Andrews E, Benjamin TL. 2014. A Mouse Polyomavirus-encoded
454 microRNA Targets the Cellular Apoptosis Pathway through Smad2 Inhibition. *Virology* 468-
455 470: 57-62.
- 456 28. Gosert R, Rinaldo CH, Funk GA, Egli A, Ramos E, Drachenberg CB, Hirsch HH. 2008.
457 Polyomavirus BK with rearranged noncoding control region emerge in vivo in renal transplant
458 patients and increase viral replication and cytopathology. *J Exp Med* 205:841–852.
- 459 29. Chen CJ, Burke JM, Kincaid RP, Azarm KD, Mireles N, Butel JS, Sullivan CS. 2014. Naturally
460 Arising Strains of Polyomaviruses with Severely Attenuated MicroRNA Expression. *J Virol*
461 88:12683-12693.
- 462 30. Swanson PA, Pack CD, Hadley A, Wang C-R, Stroynowski I, Jensen PE, Lukacher AE. 2008.
463 An MHC class Ib–restricted CD8 T cell response confers antiviral immunity. *J Exp Med*
464 205:1647–1657.
- 465 31. Gattazzo F, Molon S, Morbidoni V, Braghetta P, Blaauw B, Urciuolo A, Bonaldo P. 2014.
466 Cyclosporin A Promotes in vivo Myogenic Response in Collagen VI-Deficient Myopathic
467 Mice. *Front Aging Neurosci* 244.
- 468 32. Kemball CC, Lee ED, Vezys V, Pearson TC, Larsen CP, Lukacher AE. 2005. Late priming
469 and variability of epitope-specific CD8+ T cell responses during a persistent virus infection. *J*
470 *Immunol.*174:7950–60.
- 471

472 **Acknowledgements**

473 The work described in this article was supported by a Burroughs Wellcome Investigators in
474 Pathogenesis Award to CSS and a grant from the Cancer Prevention and Research Institute of
475 Texas [RP140842]. The authors would like to thank Dr. Lauren Ehrlich and Dr. Edward
476 Marcotte for reagents, and Dr. Luis Villarreal for insights regarding viral persistence.

477

478 **Figure Legends**

479 **Figure 1. Identification of MuPyV miRNAs by small RNA sequencing.**

480 NIH3T3 cells were infected with MuPyV-PTA at an MOI of 0.1. A small RNA library was
481 prepared 7 days p.i. Dots on the graph represent the read counts of the 5' end of small RNA reads
482 mapping to the MuPyV-PTA genome (NCBI accession number: U27812), positioned on the x-
483 axis. The arrow below the graph represents the pre-miRNA hairpin position and direction. The
484 MuPyV-PTA reference sequence encoding the miRNAs is indicated. Sequences of the three most
485 abundant small RNAs mapping to the 5-prime (bold/red) and 3-prime (bold/blue) arms of pre-
486 miRNA hairpin are shown aligned to the pre-miRNA. Numbers represent the read counts.

487 **Figure 2. Quantitation of PTA and PTA-dl1013 during the acute and persistent phases of** 488 **infection.**

489 Adult C57BL/6 female mice were inoculated with 1×10^5 IU of either PTA (white circles) or PTA-
490 dl1013 (gray circles) via IP injection, and genome levels in spleen and kidney were quantified at
491 times post infection by using a TaqMan probe and primers that recognize both genomes. The limit
492 of detection for the qPCR reactions was 10 copies. The input DNA amounts were 20 ng (at 1, 4,
493 and 10 weeks p.i.), 40 ng (at 16 weeks), or 200 ng (at 28 weeks). Genome copy numbers were
494 normalized per 1 μ g. Dots represent individual animals. The black bar represents the average
495 genome copy number. The gray bars represent the limit of detection (L.O.D.) of the assay after
496 normalization. Samples that were below the limit of detection are graphed at the limit of detection.
497 P-values were calculated using the Mann-Whitney U test.

498 **Figure 3. Quantitation of PTA and PTA-dl1013 in tissues of co-infected mice.**

499 qPCR analysis of PTA and PTA-dl1013 genome levels in the spleen, kidney, liver, and bladder of
500 adult C57BL/6 mice inoculated with 5×10^4 IUs of PTA and 5×10^4 IUs of PTA-dl1013 via IP
501 injection. Tissues were harvested at indicated time points. DNA was recovered and subject to
502 qPCR analysis using PTA- and PTA-dl1013- specific probes. The limit of detection (L.O.D.) was
503 10 copies. Samples in which PTA or PTA-dl1013 were below the limit of detection were graphed
504 at the limit of detection. The quantities were normalized to 1-ug of total DNA. P-values were
505 determined using Mann-Whitney U test.

506 **Figure 4. Ratio of PTA and PTA-dl1013 in tissues of co-infected mice.**

507 The ratio of PTA and PTA-dl1013 genome copies from (A) in the indicated organs of individual
508 mice co-infected with PTA and PTA-dl1013. Values below the limit of detection were set at the
509 limit of detection. The dots represent $\text{Log}_{10}(\text{PTA}/\text{PTA-dl1013})$. P-values were calculated using
510 one-sample t-test.

511 **Figure 5. Quantitation of PTA and PTA-dl1013 DNA shedding in the urine.**

512 Mice were co-infected with 5×10^4 IU of PTA and 5×10^4 IU of PTA-dl1013 via IP injection, urine
513 samples were collected at the indicated times, and strain-specific qPCR was used to quantify wt
514 and mutant genomes. The number of mice tested at each time ranged from 18-30 mice during days
515 1-27 p.i., 10-20 mice during days 29-55 p.i., and 4 mice during days 62-492 p.i. Panel A presents
516 a dot plot of genome equivalents of PTA (blue circles) and PTA-dl1013 (yellow triangles) in 2 ul
517 of urine from mice that shed viral genome copies equal to or greater than the limit of detection of
518 the qPCR assay. Mice that did not shed above the limit of detection or time points in which
519 genomes were not detected were not included in this analysis. Lines represent the median values

520 of PTA (solid blue) and PTA-dl1013) (dotted yellow). Significant differences ($P \leq 0.05$) between
521 PTA and PTA-dl1013 genome levels are marked by asterisks. Panel B compares the ratio of wt
522 and mutant genomes in individual mice co-infected with PTA and PTA-dl1013. When only one
523 genome could be detected (either PTA or PTA-dl1013), the other genome was set at the limit of
524 detection in order to calculate the PTA/PTA-dl1013 ratio. The line represents the average
525 $\log_{10}(\text{PTA}/\text{PTA-dl1013}) \pm \text{SEM}$. P values were calculated by using a one sample t-test (asterisks
526 indicate $P \leq 0.05$).

527 **Figure 6. Analysis of PTA and PTA-dl1013 shedding in C57BL/6 Rag2^{-/-} mice.**

528 Nine female C57BL/6-RAG2^{-/-} mice were co-infected with 5×10^4 IU of PTA and 5×10^4 IU of
529 PTA-dl1013 via IP injection. Urine was collected during the acute phase of infection, and genomic
530 DNA was quantified by strain-specific qPCR analysis. Wild type C57BL/6 mice co-infected with
531 PTA (blue circles/dashed line) and PTA-dl1013 virus (yellow triangles/dashed line) are from
532 Figure 6. PTA genomes (blue circles/solid line) and PTA-dl1013 virus (yellow triangles/solid
533 line) from C57BL/6-Rag2^{-/-} mice are presented. Plots represent the average ($\pm \text{SEM}$, n=8-9) at the
534 indicated times.

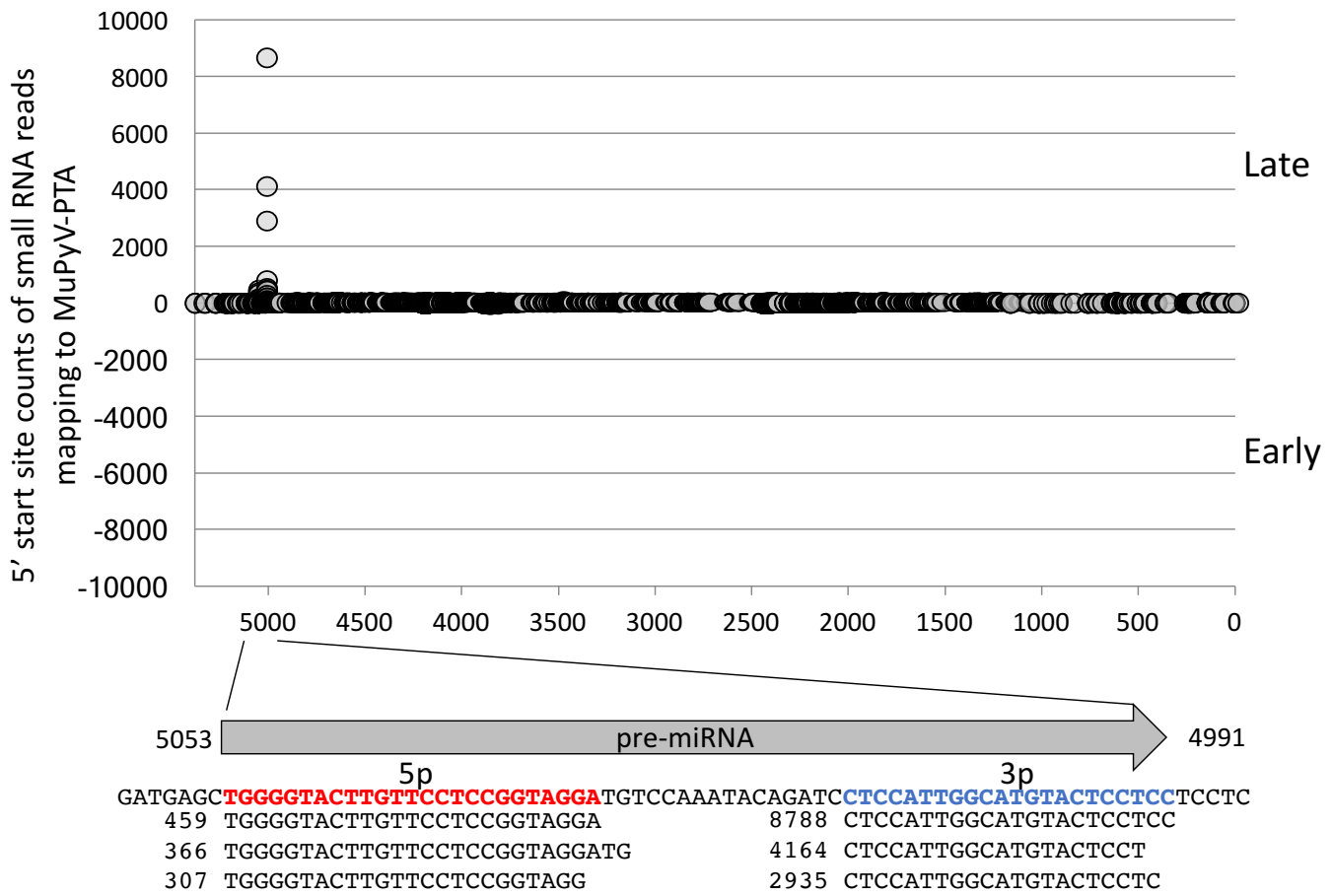


Figure 1

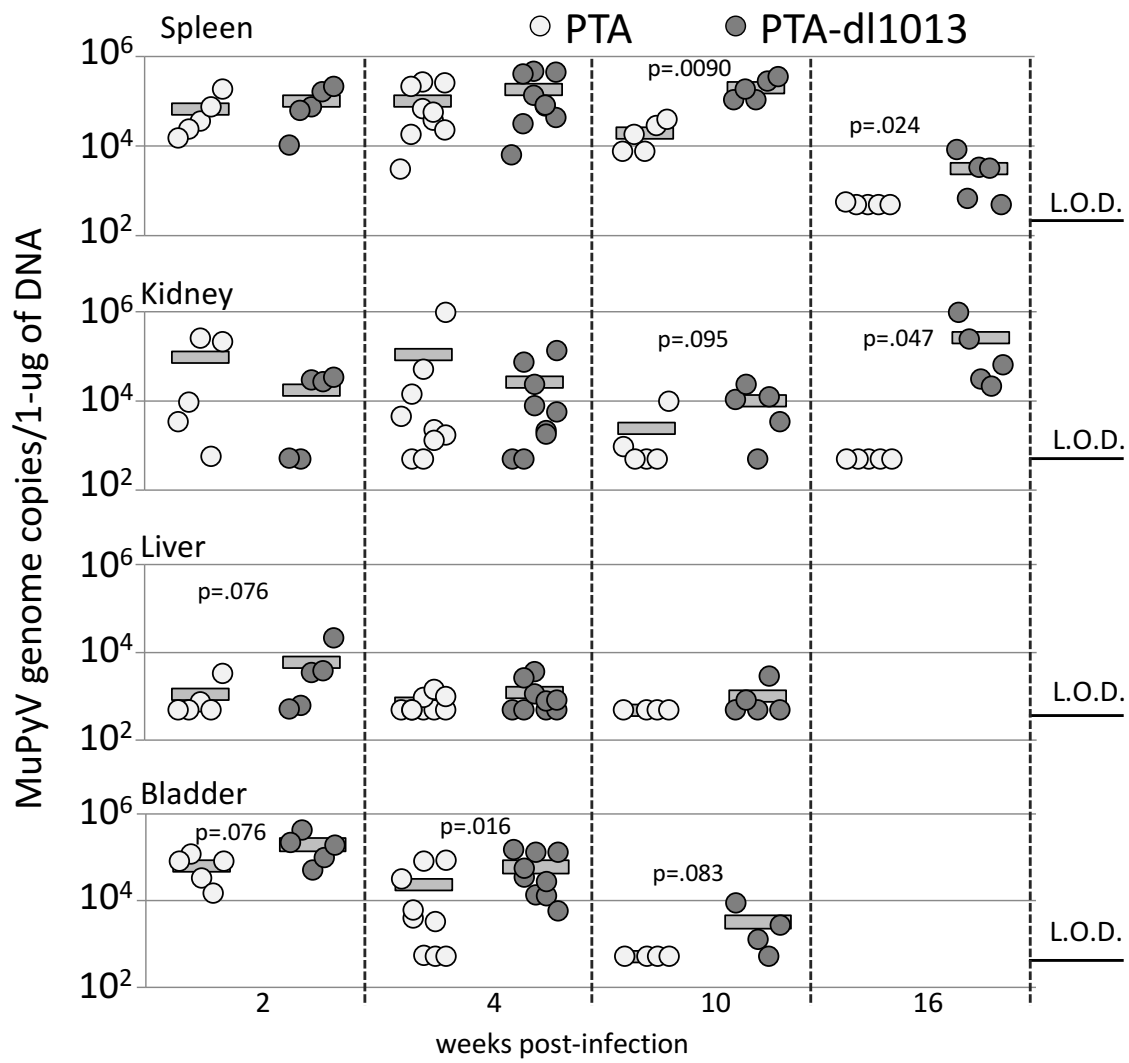


Figure 3

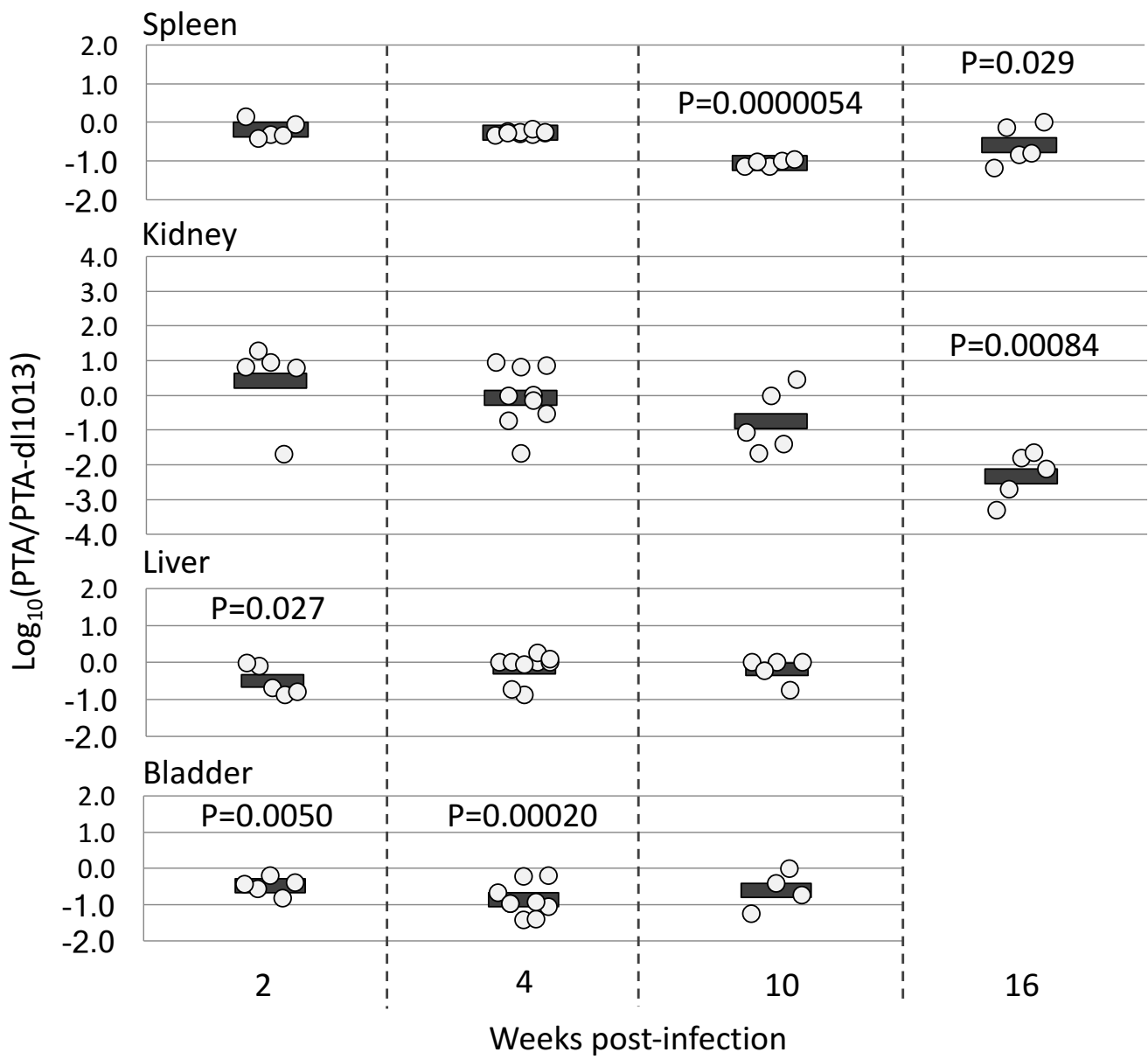


Figure 4

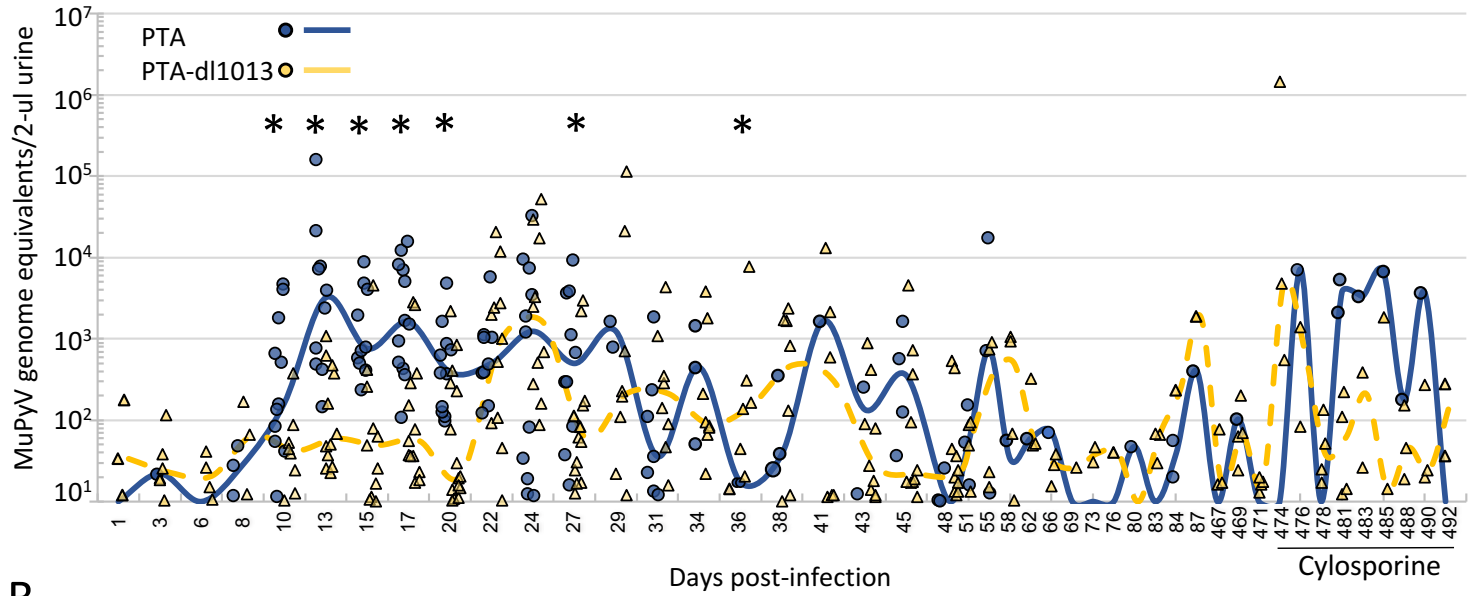
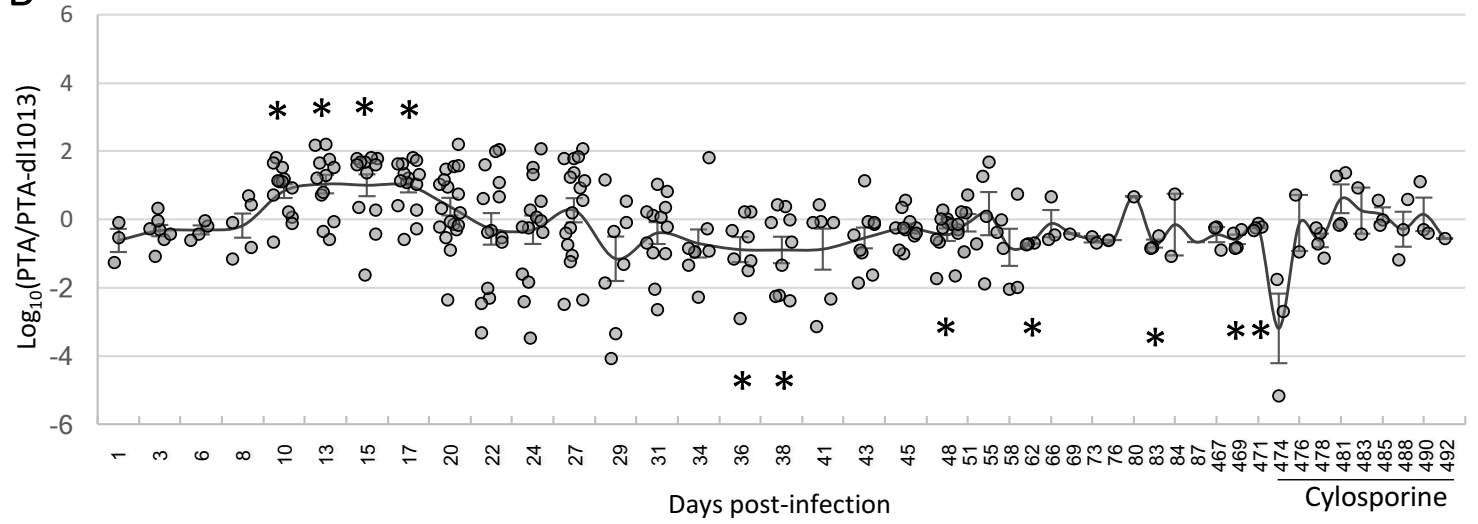
A**B**

Figure 5

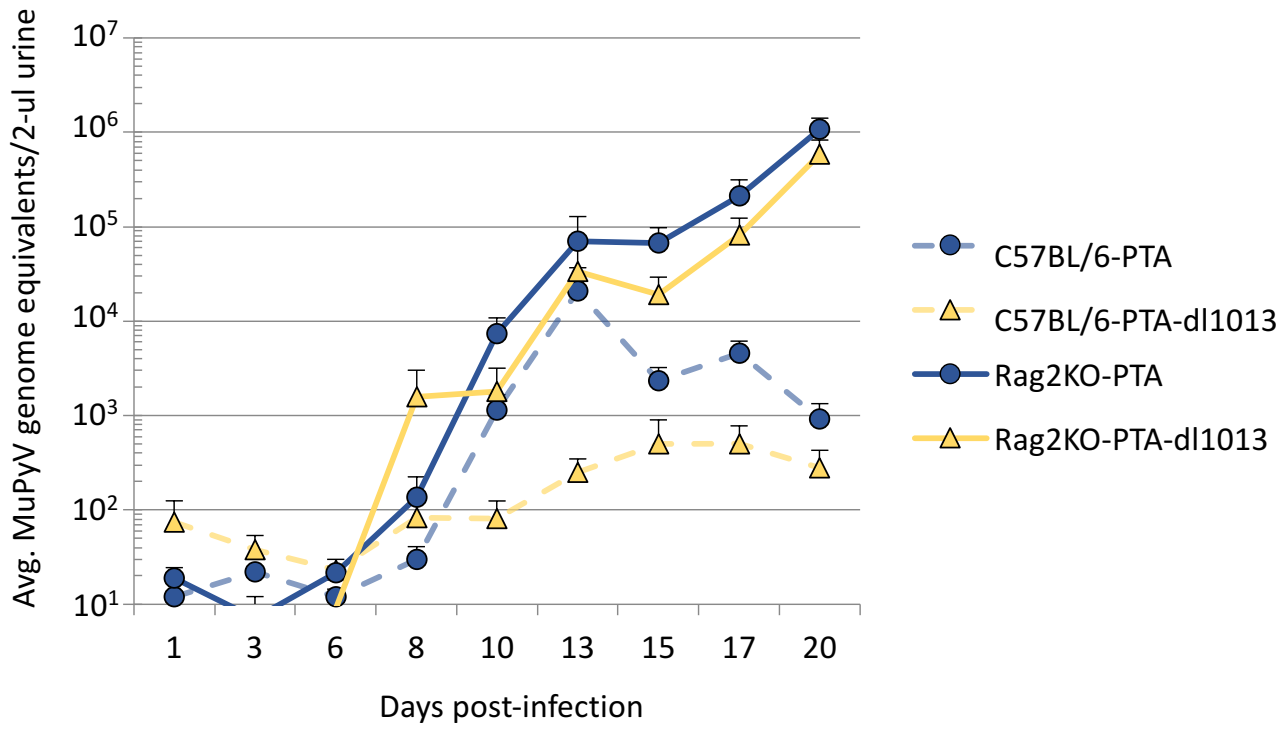


Figure 6